Chapter 6

Diffraction

6.1 The Geometrical theory of diffraction

The geometrical theory of optics has eversince its emergence been a very useful tool in describing the evolution of waves in terms of rays. Starting in 1959 Keller strongly improved this theory by extending it to include diffraction effects. In a series of papers [38] he introduced and developed the geometrical theory of diffraction describing the well known wave phenomena ranging from diffraction around smooth objects to diffraction on vertices and edges. He tested the theory on several examples and observed an excelent agreement with experiments and theoretical results obtained by direct wave mechanics.

In this section we first start by a brief review of the ordinary theory of geometrical optics whereafter we describe Kellers construction of the geometrical theory of diffraction.

In geometrical optics the aim is to describe the electromagnetic field under the assumption that the field propagates along *rays*. The rays are determined by the *principle of least action* or the Fermat principle which states that among all trajectories between two points A and B, only the paths of least travel time should give a contribution to the resulting field.

In the ordinary theory of geometrical optics a field value is associated with each ray. The field is composed of a phase function $\phi(s)$ and an amplitude $A(s)$ which are both functions of the distance s along the ray. The phase is just a linear function of the distance: $\phi(s) = \phi_0 + s$, which follows from the optical law $d\phi/ds = 1$. The initial phase ϕ_0 is the phase at the point from which the distance s is measured. The amplitude is determined by conservation of energy along the ray. For a tube of rays the energy flux is the same through every cross section of the tube. If the amplitude and cross section area at some point in the tube is given by A_0 and $d\sigma_0$ and by A and $d\sigma$ at some later point, then the principle of conservation of energy states that $A_0^2 d\sigma_0 = A^2 d\sigma$ and hence the amplitude is given by $A = A_0 \sqrt{d\sigma_0/d\sigma}$. To calculate the field at some point P we just follow all the rays that emerge from the source Q (or sources) and

impinges at the final point under investigation. The resulting field $u(P)$ is then the sum of the contributions from the different paths p:

$$u(P) \;=\; \sum_p A_p e^{ik(s+\phi_0)} \tag{6.1}$$

where $k = \omega/c$ is the wavenumber, ω is the angular frequency of the field and c is its propagation speed. At this point we have only described the evolution of a scalar field, but for a vector field the description is completely analogous. For simplicity we shall here continue to treat scalar fields.

The next step is to calculate the area ratio $d\sigma_0/d\sigma$. To do this, consider figure 6.1. Since $d\sigma_0$ and $d\sigma$ are just the areas cut out by the tube at the
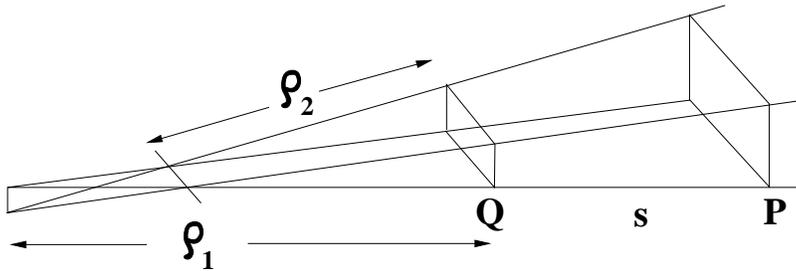

Figure 6.1: A tube of rays emerging from Q and impinging at P. The principal radii of curvature are indicated as ρ_1 and ρ_2.

wavefronts $\phi = \phi_0$ and $\phi = \phi_0 + s$, and since the rays are just straight lines we obtain by simple geometry

$$\frac{d\sigma_0}{d\sigma} = \frac{\rho_1 \rho_2}{(\rho_1 + s)(\rho_2 + s)} \tag{6.2}$$

and hence the field contribution from a single ray at the point P is just

$$u(P) \;=\; A_0 \left(\frac{\rho_1 \rho_2}{(\rho_1 + s)(\rho_2 + s)} \right)^{1/2} e^{ik(\phi_0 + s)} \tag{6.3}$$

In two dimensions the result would be the same except for the first factor in both nominator and denominator. This specific result holds only for free propagation, but can easily be generalised to include specular reflections from smooth surfaces by introducing an effective traveled distance. The above results contain the essence of the ordinary theory of geometrical optics.

Next we shall use the above ideas to describe diffraction from the exterior of a smooth convex body. Besides the straight line rays from the usual geometrical optics theory we then need additional diffraction rays. These are introduced by an extention of Fermat's principle stating that the diffracted rays connecting

two points Q and P are those curves which have stationary length among all the topologically different curves joining Q and P. From this principle it follows, that in a homogeneous medium the rays will be straight lines for the free flight and that they will follow the geodesics on the surface of the obstacles on which they diffract. An example of such a ray is shown on figure 6.1. From the usual
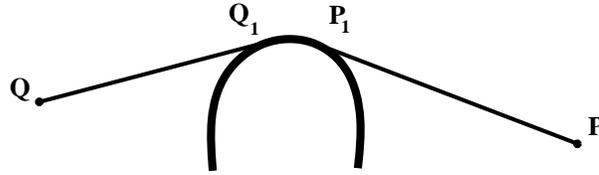

Figure 6.2: A diffracted ray from a point Q to P. The points Q_1 and P_1 are the points where the straight line ray hits the obstacle tangentially and creates the diffracted ray, and where the diffracted ray leaves the obstacle by acting like a source for a new straight line trajectory. The ray is seen to be the shortest among all the continuous curves joining Q and P by passing over the obstacle.

geometrical optics described above we can easily get the field value at the point where the ray impinges. We now *assume* that the field on the diffracted (or surface) ray at the point Q_1 is proportional to the incident field

$$A_d(Q_1) \quad = \quad D(Q_1)A_i(Q_1) \tag{6.4}$$

where we have defined the *diffraction coefficient* $D(Q_1)$, which we assume depends only on the nature of the field, the local properties of the obstacle at Q_1 and the wavenumber k. In cases where boundary conditions requires that the field be identically zero at the surface of the obstacle (as for instance hard wall potentials in quantum mechanics) the result is the same except that the diffracted field u_d must be interpreted as a measure of the typical size of the field in the vicinity of the surface. The diffraction constant is determined by comparison to the exact field solution for some simple geometry. We postpone this calculation till section 6.3.

Next step is to get the variation of the field along the surface ray. If we let t denote the distance traveled along the surface of the obstacle then the previous considerations yields for the phase: $\phi_d(t) = \phi_i(Q_1) + t$. To determine the amplitude as function of t we apply the principle of energy conservation along a narrow strip of geodesics on the surface of the obstacle containing the surface ray (see figure 6.1).

We denote the width of the strip $d\sigma(t)$ and the energy flux through a cross
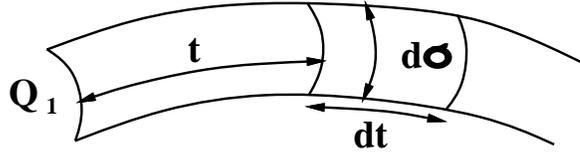
Figure 6.3: A strip of diffracted rays moving along the geodesics of the surface of the obstacle.

section of the strip is then proportional to $A_d^2(t)d\sigma(t)$. At a slightly later time the energy flux through the cross section $d\sigma(t + dt)$ will be smaller because diffracted rays have been shed out in the meantime. We assume that the radiated energy is proportional to dt, $d\sigma(t)$ and to the square of the amplitude $A_d(t)^2$. The energy conservation requires

$$A_d^2(t + dt)d\sigma(t + dt) - A_d^2(t)d\sigma(t) = -2\alpha(t)A_d^2(t)d\sigma(t)dt \qquad (6.5)$$

where we have introduced the proportionality constant $2\alpha(t)$ relating the energy flux to the radiated energy. As in the case of the diffraction coefficient we expect that $\alpha(t)$ depends of the local properties of the obstacle and of the nature of the field. The determination of $\alpha(t)$ takes place in the same way as that of D, and will also be postponed untill section 6.3. (6.5) yields a differential equation for the time dependance of the amplitude

$$\frac{d}{dt}(A_d^2(t)d\sigma) = -2\alpha(t)A_d^2d\sigma \qquad (6.6)$$

which immediately yields

$$A_d(t) = A_d(0)\left(\frac{d\sigma_0}{d\sigma}\right)^{1/2}\exp\left(-\int_0^t \alpha(\tau)d\tau\right). \qquad (6.7)$$

Here $d\sigma_0/d\sigma$ is the ratio with which the geodesics spread out over the surface of the obstacle. If for instance the geodesics are parallel, this ratio would simply be unity - a case we shall encounter in the 2-dimensional description where the width of the strip is constant equal zero. The diffracted field on the surface of the obstacle at distance t from Q_1 thus reads

$$u_d(t) = D(Q_1)A_i(Q_1)\left(\frac{d\sigma_0}{d\sigma}\right)^{1/2}\exp\left(ik(\phi_i(Q_1) + t) - \int_0^t \alpha(\tau)d\tau\right) \quad (6.8)$$

From (6.8) we get the field at the point P_1. To get the field at P we should make use of the usual geometrical optics propagation. However this is not directly

applicable because at P_1 the field acts like a source implying that one of the principal radii of curvature is zero. We make use of a limiting procedure where we determine the field at P as function of the field at a variable point x on the line connecting P_1 with P. Letting x tend to P_1 we then obtain the field at P by demanding this to be constant during this procedure. As x tends to P_1 we have the following scenario: ρ_2 tends to zero, ρ_1 tends to some finite value, ϕ_0 tends to $\phi_d(P_1)$ and s tends to the distance from P_1 to P while $u(P)$ remains constant. It then follows from (6.3) that A_0 must tend to infinity in such a way that $A_0\sqrt{\rho_2}$ converges to a finite limit. Denoting this limit $A'_d(P_1)$ we can write the field at P

$$u_d(P) \;=\; A'_d(P_1) \left(\frac{\rho_1}{s(\rho_1+s)}\right)^{1/2} \exp(ik(\phi_d(P_1)+s)) \tag{6.9}$$

We assume now that $A'_d(P_1)$ is proportional to the diffracted field at P_1 so that $A'_d(P_1) = D(P_1)u_d(P_1)$ and that the diffraction constant $D(P_1)$ is *the same* function of the local properties of the obstacle and of the field as the diffraction constant at Q. This assumption is based on the reciprocity principle which states that a source at Q produces the same field at P as a source located at P would produce in Q. We can now write the field at P as

$$
\begin{aligned}
u_d(P) \;=\;& A_i(Q_1)D(P_1)D(Q_1) \left(\frac{d\sigma(Q_1)}{d\sigma(P_1)}\right)^{1/2} \left(\frac{\rho_1}{s(\rho_1+s)}\right)^{1/2} \\
\times\;& \exp\left(ik(\phi_i(Q_1)+t+s) - \int_0^t \alpha(\tau)d\tau\right)
\end{aligned}
\tag{6.10}
$$

In the derivation we have excluded fields which are required by boundary conditions to vanish on the surface of the obstacle. This is due to the fact that we have considered the amplitude function on the surface A_d. However, since the surface of the obstacle is a caustic for the diffracted field it follows that the field is much stronger in a surface layer some few wavelengths thick than it is at points further away from the surface. Therefore the discussion still holds if we interpret A_d as a measure of the field amplitude in this layer. The field within the caustic layer will have a certain profile variation with the distance along the direction of a surface normal. The amplitude at any point of the profile (except where this has a zero) can serve as a measure of the field amplitude in the caustic layer. In general it turns out to be practical at this point to expand the field in a basis of *modes* each with its own profile. Each mode will also be characterized by its own amplitude A_{dm} and its own diffraction constant $D_m(Q_1)$. According to the principle of superposition the total field must be the sum over contributions from each mode

$$
\begin{aligned}
u_d(P) \;=\;& A_i(Q_1) \left(\frac{d\sigma(Q_1)}{d\sigma(P_1)}\right)^{1/2} \left(\frac{\rho_1}{s(\rho_1+s)}\right)^{1/2} \\
\times\;& \sum_m D_m(P_1)D_m(Q_1) \exp\left(ik(\phi_i(Q_1)+t+s) - \int_0^t \alpha_m(\tau)d\tau\right)
\end{aligned}
\tag{6.11}
$$

Equation (6.12) yields the final expression for the field contribution associated with a single diffracted ray. The total field at P will then be the sum over all

rays, both usual geometric and diffracted, passing through P

$$u(P) \quad = \quad u_g(P) + u_d(P). \tag{6.12}$$

Expression (6.12) is the general result of the geometrical theory of diffraction, with the diffraction coefficients D_m and the decay constants α_m to be determined for the explicit problem under investigation. In the next section we shall see how this can be done for the 2-dimensional 1-disk problem.

6.2 The 1-disk Keller propagator

In this section we will construct a semiclassical expression for the energy domain quantum propagator in the simple 2-dimensional 1-disk scattering system using Keller's geometrical theory of diffraction together with the usual geometrical optics. Having done this, the next step will be to determine the diffraction coefficients $D(Q_1)$ and the proportionality constant α. This we will do by comparing the semiclassical expression to the semiclassical expansion of the quantum mechanical *exact 1-disk propagator*.

We consider a disk of radius a centered at the origin of a polar coordinate system (r, θ). Assuming that the disk represents an infinite potential implies that the wave function should vanish at the surface of the disk. The Greens function or propagator of the system therefore fulfills

$$(\Delta + k^2)G(\vec{r}, \vec{r}'; k) \quad = \quad \delta(\vec{r} - \vec{r}') \tag{6.13}$$

with Dirichlet boundary conditions on the surface of the disk. At $\vec{r}$ we place a wave or ray source and then try to determine the field at the receiver located at $\vec{r}'$. The geometry of the system is shown in figure 6.2. Since the operator in equation (6.13) is self adjoint we must furthermore have that the propagator is symmetric in its arguments [34]

$$G(\vec{r}, \vec{r}') \quad = \quad G(\vec{r}', \vec{r}) \tag{6.14}$$

We consider the case where the point of the observer is in the lit region of the source since this also covers the case where the observer is in the shadow region relative to the source. To obtain the field at the points of tangential incidence we use the 2-dimensional version of (6.3). If R is the distance from the source to this point we obtain

$$G_i \quad = \quad \frac{i}{4}(\frac{2}{k\pi R})^{1/2}e^{ikR-i\pi/4} \tag{6.15}$$

where we have chosen the constant in front so that G_i represents the short-wave limit of the field from a source of unit strength i.e. a source for which $-iH_0^{(1)}(kR)/4$ is the exact solution.

From (6.4) it follows that the diffraction constant $D(Q_1)$ is dimensionless and therefore if it depends on the wavenumber k it must do so in a dimensionless combination ka where a has the dimension of length. We shall let a be the local
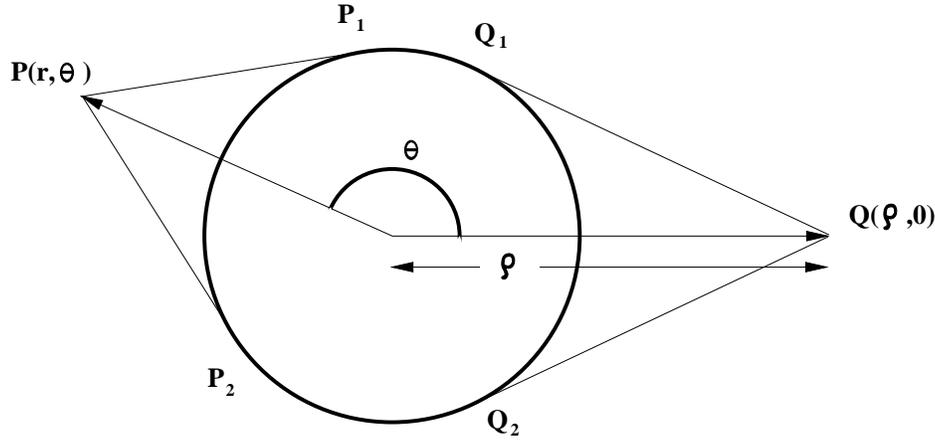
Figure 6.4: The geometry of the disk and the source. The two families of rays going from the source Q to the receiver P are shown.

radius of curvature at the point where the ray impinges. One might expect that a detailed description of $D(Q_1)$ would include all kinds of derivatives of the surface, but we shall assume from now that to the leading order $D(Q_1)$ only depends on the local properties of the obstacle through this combination. The decay exponent α which has the dimension 1/length we shall also assume depends only on k and on the local radius of curvature even though small correction terms might depend on other geometrical properties of the surface. Under these assumptions it should be possible to determine the leading terms in D_m and α_m from the field diffracted by any simple shape.

The geodesics on the surface of the circle are simply arcs of the circle implying that the ratio $d\sigma(Q_1)/d\sigma(t)$ is unity since the tube of rays cannot spread into the direction orthogonal to the plane. Further more because the wavefronts on the surface of the cylinder are simply points the radius of curvature ρ_1 is infinite so that $(\rho_1/(\rho_1+s))^{1/2}$ obtains its limitting value $s^{1/2}$ in the expression (6.12). Also, since the radius of curvature is constant, the diffraction coefficients and the decay exponent will be constants. Using (6.15) for the incident field and for the field leaving the disk and hitting the receiver we obtain by applying the above considerations

$$
\begin{aligned}
G_d(\vec{r},\vec{r}') &= (8\pi k)^{-1}[(r^2 - a^2)(r'^2 - a^2)]^{-1/4}\exp\{ik[(r'^2 - a^2)^{1/2} + (r^2 - a^2)^{1/2}] \\
&+ \frac{i\pi}{2}\}\sum_m D_m^2 e^{(ik-\alpha_m)t}
\end{aligned}
\tag{6.16}
$$

Equation (6.16) gives the value of the field at P associated with any ray from Q that creeps along the surface of the cylinder a distance t. As we see there are two families of rays. The first family follows the straight line QP_1 winds around the disc a number of times and then follows the straight line Q_1P. The second family follows the path $QP_2(windings)Q_2P$. For the first family t takes the values $t_n = t_0 + 2n\pi a$ where $t_0 = a(2\pi + \theta) - a\cos^{-1}(a/r) - a\cos^{-1}(a/r')$ and θ is the angle between the source and the observer. In case of the existence of more

than one obstacle of course one or both of the families might be nonexisting. Inserting these values of t_n, the expression (6.16) becomes a geometrical series and we obtain for the first family

$$
\begin{aligned}
G_d^{(1)}(r,\theta) &= (8\pi k)^{-1}(r^2 - a^2)^{-1/4}(r'^2 - a^2)^{-1/4} \\
&\times \exp\{ik([r'^2 - a^2]^{1/2} + [r^2 - a^2]^{1/2} + \frac{i\pi}{2}\} \\
&\times \sum_m D_m^2 e^{(ik-\alpha_m)t_0}[1 - \exp\{2\pi(ika - a\alpha_m)\}]^{-1}.
\end{aligned}
\tag{6.17}
$$

For the second family everything is the same except that $(2\pi + \theta)$ is replaced by $2\pi - \theta$ and adding the contributions from both families we get

$$
\begin{aligned}
G_d(r,\theta) &= (8\pi k)^{-1}(r^2 - a^2)^{-1/4}(r'^2 - a^2)^{-1/4} \\
&\times \exp\{ik([r'^2 - a^2]^{1/2} + [r^2 - a^2]^{1/2} + \frac{i\pi}{2}\} \\
&\times \sum_m D_m^2 \frac{\exp\{(ika - a\alpha_m)(2\pi + \theta)\} + \exp\{(ika - a\alpha_m)(2\pi - \theta)\}}{1 - \exp\{2\pi(ika - a\alpha_m)\}} \\
&\times \exp\{-(ika - a\alpha_m)[\cos^{-1}(a/r) + \cos^{-1}(a/r')]\}
\end{aligned}
\tag{6.18}
$$

Equation (6.18) is the final Keller expression for the field at P caused by the source at Q in the frame of the geometrical theory of diffraction. As we see the reciprocity condition (6.14) is automatically fulfilled as it should, and we note that the Greens function has the structure

$$
G_d = G_{free}G_{diff}G_{free}.
\tag{6.19}
$$

What is left to be done is to compare this expression to the expansion of the exact solution of the propagator of the problem for large ka to determine the coefficients D_m and α_m. An expression for such an expansion we shall obtain in the following section.

6.3   The exact 1-disk propagator

In the following derivations we shall mainly follow the work of Franz [28] and the excellent rewiev notes by A. Wirzba [63]. As above we assume that the disk is centered at the origin in the two-dimensional plane, and we introduce the usual polar coordinate system (r, θ). The stationary 1-disk problem therefore corresponds to the Helmholtz equation in 2 dimensions

$$
\left(\frac{\partial^2}{\partial r^2} + \frac{1}{r}\frac{\partial}{\partial r} + \frac{1}{r^2}\frac{\partial^2}{\partial \theta^2} + k^2\right)u(r,\theta) = 0
\tag{6.20}
$$

(with $k = \sqrt{2mE}/\hbar$). Since we are interested in scattering off a hard wall we impose the Dirichlet boundary condition $u(r,\theta)|_{r=a} = 0$. The free energy-domain Greens function of the problem is given by [28]

$$
G_0(k|\vec{r}' - \vec{r}|) = -\frac{i}{4}H_0^{(1)}(k|\vec{r}' - \vec{r}|)
\tag{6.21}
$$

$$= -\frac{i}{4} \sum_{m=-\infty}^{+\infty} e^{im\theta} H_m^{(1)}(kr') J_m(kr) \quad \text{for } r' > r, \qquad (6.22)$$

where θ is the angle between $\vec{r}'$ and $\vec{r}$.

As the 1-disk scattering problem is separable the full propagator can be simply constructed by splitting J_m in the free propagator expression in an incoming and outgoing Hankel function and imposing the boundary conditions

$$J_m(kr) = \frac{1}{2}(H_m^{(1)}(kr) + H_m^{(2)}(kr))$$

where the asymptotically outgoing Hankel function $H_m^{(1)}(kr)$ obtains a scattering phase from the boundary condition $G = 0$ on the surface

$$H_m^{(2)}(ka) + S_{mm} H_m^{(1)}(ka) = 0 \Rightarrow$$

$$S_{mm} = -\frac{H_m^{(2)}(ka)}{H_m^{(1)}(ka)} \quad \text{Dirichlet b.c.} \quad (6.23)$$

We can therefore write the 1-disk Greens function as

$$G(k\vec{r}', k\vec{r}) = -\frac{i}{8} \sum_{m=-\infty}^{+\infty} e^{im\theta} H_m^{(1)}(kr') \left(H_m^{(2)}(kr) + S_{mm} H_m^{(1)}(kr) \right) (6.24)$$

where the scattering matrix $S_{mm'} = \delta_{mm'} S_{mm}$ contains the boundary condition. As for $kr \gg 1$ the number of contributing terms in the sum in (6.24) becomes bigger and bigger the result is only useful for small values of kr. Our aim is to find a numerical useful result also for large values of kr. Such an expression can be obtained by following the work of Franz [28] and use the Watson resummation method [58] which leads to an asymptotic expansion of the field. The idea here is to write the sum (6.24) as a contour integral in the complex plane and obtain the individual terms as the residues of a suitable function. More explicitly we have

$$\sum_{m=-\infty}^{+\infty} f(m) = \oint_C d\nu \frac{f(\nu)}{e^{i2\pi\nu} - 1} = \oint_C d\nu \frac{e^{-i\pi\nu} f(\nu)}{2i \sin(\nu\pi)} , \qquad (6.25)$$

where the path C encircles counterclock-wise the real ν-axis. This resummation is valid in case $f(\nu)$ is holomorphic in the strip D which covers the real ν-axis, i.e. $\delta D = C$.

Using the Watson resummation the 1-disk propagator yields

$$G(k\vec{r}', \vec{r}) = -\frac{i}{8} \oint_C d\nu \frac{e^{i\nu(\theta-\pi)}}{2i \sin(\nu\pi)} H_\nu^{(1)}(kr') \left(H_\nu^{(2)}(kr) + S_{\nu,\nu} H_\nu^{(1)}(kr) \right)$$

$$(6.26)$$

The contour C can be transformed to a path above the real ν-axis

$$-\frac{i}{8} \oint_C d\nu \chi_\nu = -\frac{i}{8} \int_{+\infty+i\epsilon}^{-\infty+i\epsilon} d\nu \chi_\nu - \frac{i}{8} \int_{-\infty-i\epsilon}^{+\infty-i\epsilon} d\nu \chi_\nu$$

$$= +\frac{i}{8} \int_{-\infty+i\epsilon}^{+\infty+i\epsilon} d\nu \chi_\nu - \frac{i}{8} \int_{-\infty+i\epsilon}^{+\infty+i\epsilon} d\nu \chi_{-\nu} \qquad (6.27)$$

where the integration variable ν has been changed to $-\nu$ in the last term. Using the rules $H^{(1)}_{-\nu}(kr) = \exp(i\nu\pi)H^{(1)}_{\nu}(kr)$ and $H^{(2)}_{-\nu}(kr) = \exp(-i\nu\pi)H^{(2)}_{\nu}(kr)$ for the Hankel functions we find the following form of the one-disk Greens function

$$G(k\vec{r}',k\vec{r}) \;\; = \;\; -\frac{i}{8}\int_{-\infty+i\epsilon}^{+\infty+i\epsilon} d\nu \frac{\cos(\nu(\theta-\pi))}{2i\sin(\nu\pi)}H^{(1)}_{\nu}(kr')\left(H^{(2)}_{\nu}(kr) + S_{\nu\nu}H^{(1)}_{\nu}(kr)\right).$$

(6.28)

We now have the following three possible situations: (a) $\vec{r}$ lies in the "shadow region" of $\vec{r}'$ with respect to the disk; (b) $\vec{r}$ lies in the lit region, and (c) $\vec{r}$ lies on the boundary of the lit and the shadow region. We will exclude the latter case since in the two- and three-disk cases which we are mostly interested in there are no grazing contributions for the corresponding diffractional rays. This case has to be handled with different methods than the ones presented here. Further more the situation (a) is a special case of case (b) since they will both have diffractional terms whereas in case (b) there will also be a direct and a reflected ray. We shall therefore in the following deal only with case (b) i.e. the lit region. This case also corresponds to the semiclassical derivation above using the Keller construction. The creeping angles can be immediately obtained as

$$\alpha^{(-)}_n \;\; = \;\; 2\pi - \theta - \arccos\frac{a}{r'} - \arccos\frac{a}{r} + 2\pi n$$

(6.29)

$$\alpha^{(+)}_n \;\; = \;\; 2\pi + \theta - \arccos\frac{a}{r'} - \arccos\frac{a}{r} + 2\pi n$$

(6.30)

and are positive for any $n = 0, 1, 2, \ldots$. As in the Keller construction the index n parameterizes the fact that the creeping ray can wind around the disk n times before leaving it. The prefactor in (6.28) can be written as

$$\frac{\cos(\nu(\theta-\pi))}{i\sin(\nu\pi)} = -\frac{e^{i\nu(2\pi+\theta)}}{1-e^{i2\nu\pi}} - \frac{e^{i\nu(2\pi-\theta)}}{1-e^{i2\nu\pi}} - e^{i\nu\theta}\;.$$

(6.31)

Note that the last term does not contain any poles on the real axis any longer, as we shall see this term will contribute only to the direct and reflected ray contributions in the semiclassical approximation. We can therefore write

$$G(k\vec{r},k\vec{r}') = G_{\mathrm{geo}}(k\vec{r},k\vec{r}') + G_{\mathrm{creep}}(k\vec{r},k\vec{r}')$$

(6.32)

with

$$G_{\mathrm{geo}}(k\vec{r},k\vec{r}') \;\; = \;\; -\frac{i}{8}\int_{-\infty+i\epsilon}^{+\infty+i\epsilon} d\nu\, e^{i\nu\theta}\left(H^{(1)}_{\nu}(kr')H^{(2)}_{\nu}(kr) - H^{(1)}_{\nu}(kr')\frac{H^{(2)}_{\nu}(ka)}{H^{(1)}_{\nu}(ka)}H^{(1)}_{\nu}(kr)\right)$$

,

(6.33)

$$G_{\mathrm{creep}}(k\vec{r},k\vec{r}') \;\; = \;\; -\frac{i}{8}\int_{-\infty+i\epsilon}^{+\infty+i\epsilon} d\nu\, \frac{e^{i\nu(2\pi+\theta)} + e^{i\nu(2\pi-\theta)}}{1-e^{i2\nu\pi}}H^{(1)}_{\nu}(kr')$$

$$\times\frac{H^{(2)}_{\nu}(kr)\;H^{(1)}_{\nu}(ka) - H^{(2)}_{\nu}(ka)H^{(1)}_{\nu}(kr)}{H^{(1)}_{\nu}(ka)}\;,$$

(6.34)

where we have splitted up the Greens function in a pure geometrical term corresponding to the ordinary geometrical theory of diffraction and into a pure

diffractional or creeping term corresponding to the new introduced diffractional rays propagating on the surface of the obstacle. The semiclassical evaluation of these two contributions will be quite different. In the following we shall investigate the two cases in some detail.

6.3.1   The geometrical contribution

In this paragraph we shall account for the geometrical part of the semiclassical expression of the propagator. The expression for the geometrical part reads

$$G_{\text{geo}}(k\vec{r}, k\vec{r}') \quad = \quad -\frac{i}{8} \int_{-\infty + i\epsilon}^{+\infty + i\epsilon} d\nu\, e^{i\nu\theta} \left(H_\nu^{(1)}(kr') H_\nu^{(2)}(kr) - H_\nu^{(1)}(kr') \frac{H_\nu^{(2)}(ka)}{H_\nu^{(1)}(ka)} H_\nu^{(1)}(kr) \right)$$

As we see the expression does not contain the Watson denominator so we are free to deform the integration path across the real axis. However the integral cannot be substituted by a residua sum because there is no damping term ensuring that the integrant vanishes at infinity. Before evaluating the integral we note that we can split up the expression further into the first part which is independant of a and which therefore can only contain information about the direct geometrical contribution, and into the second term which then turns out to contain the reflection contribution. The semiclassical evaluation of the summands will now consist in first inserting the Debye approximation for the Hankel functions

$$H_\nu^{(1)}(kr) \sim \sqrt{\frac{2}{\pi \sqrt{(kr)^2 - \nu^2}}} \exp\left(i\sqrt{(kr)^2 - \nu^2} - i\nu \arccos \frac{\nu}{kr} - i\frac{\pi}{4} \right)$$

$$(6.35)$$

$$H_\nu^{(2)}(kr) \sim \sqrt{\frac{2}{\pi \sqrt{(kr)^2 - \nu^2}}} \exp\left(-i\sqrt{(kr)^2 + \nu^2} - i\nu \arccos \frac{\nu}{kr} + i\frac{\pi}{4} \right)$$

$$(6.36)$$

which is valid for $(kr)^2 > \nu^2 \gg 1$. Second we shall evaluate the resulting integrals via the saddlepoint approximation where the saddles are located on the real ν axis. The result of this procedure yields (see appendix 9.2 for details)

$$G_{\text{geo}}(k\vec{r}, k\vec{r}') \quad \simeq \quad -\frac{i}{4} \sqrt{\frac{2}{\pi}} \frac{e^{iL_{\text{direct1}} - i\pi/4}}{\sqrt{kL_{\text{direct1}}}} + \frac{i}{4} \sqrt{\frac{2}{\pi}} \frac{e^{ikL_{\text{refl}} - i\pi/4}}{\sqrt{kR_{\text{eff}}}} \qquad (6.37)$$

where $L_{\text{direct1}} = \sqrt{(kr')^2 - \nu_{S1}^2} - \sqrt{(kr)^2 - \nu_{S1}^2} = |\vec{r}' - \vec{r}|$ is the geometrical distance between $\vec{r}'$ and $\vec{r}$, and where

$$L_{\text{refl}} \quad = \quad d' + d \qquad\qquad\qquad\qquad\qquad (6.38)$$

$$R_{\text{eff}} \quad = \quad d' + d + \frac{2dd'}{\sqrt{a^2 - b^2}}$$

$$= \quad d' + d + \frac{2dd'}{a \cos \varphi} \qquad\qquad\qquad (6.39)$$

with

$$
\begin{aligned}
d' &\equiv \sqrt{r'^2 - b^2} - \sqrt{a^2 - b^2} \\
d &\equiv \sqrt{r^2 - b^2} - \sqrt{a^2 - b^2} \\
b &\equiv a|\sin\varphi| \ ,
\end{aligned}
$$

where φ is the angle of incidence measured with repect to the normal at the point of reflection. The parameter b thus becomes the usual impact parameter known from scattering theory.

Note that the result (9.61) is exactly what we get if we insert the semiclassical Debye approximation in the expression (6.21) for the free propagator, as it also should in the semiclassical limit $kr \gg 1$.

Modulo a sign change (which takes into account the Dirichlet boundary condition at the disk) the reflection contribution of the semiclassical propagator (9.63) has the same structure as the semiclassical direct piece (9.61), the only difference being that the length L_{direct1} is replaced by L_{refl} in the exponent and by R_{eff} in the denominator. The quantity L_{refl} is just the length of the reflected ray between $\vec{r}'$ and $\vec{r}$, whereas R_{eff} is the effective radius which determines the strength of a corresponding ray bundle. It takes into account that a ray bundle which starts at $\vec{r}'$ spreads not only according to the passed distance $L_{\mathrm{refl.}}$, but gets a further spreading by the reflection on the concave surface of the disk. If we compare the effective radius to what we get when we use the formula for the development of the Sinai Bunimovich curvatures in a single bounce

$$
\begin{aligned}
\Lambda &= l_0 \prod_{i=1}^{n_{bounce}} (1 + l_i \kappa_i^+) \\
&= l_0 \left(1 + l_1 \left(\frac{1}{l_0} + \frac{2}{a\cos\varphi}\right)\right) \\
&= l_0 + l_1 + \frac{2 l_0 l_1}{a\cos\varphi} \\
&= R_{\mathrm{eff}}
\end{aligned}
\tag{6.40}
$$

where κ_i^+ is the curvature right after the i'th bounce

$$
\kappa_i^+ = \kappa_i^- + \frac{2}{a\cos\varphi_i} \quad , \quad \kappa_i^- = \frac{\kappa_{i-1}^+}{l_i \kappa_{i-1}^+ + 1}.
\tag{6.41}
$$

The effective radius is then nothing else than the usual stabilities which we can obtain from the Jacobian of the flow 2.12.

6.3.2 The diffraction case

Let us now turn to the evaluation of the creeping terms (6.34). The creeping terms still contains the denominator $(1 - e^{i2\nu\pi})$ and the integration path can therefore not be deformed on the real axis. However, since the creeping angles are all positive they lead to an exponential damping $\exp(i\nu\alpha_n^{\pm})$ in the semiclassical limit and the path can be deformed in the upper half plane and the

integral replaced by a convergent sum of the residua i.e. the zeros of the Hankel function $H_\nu^{(1)}(ka)$. The creeping parts of the 1-disk Greens function therefore becomes

$$G_{\text{creep}}(k\vec{r}, k\vec{r}') = -\frac{1}{8i} \sum_{l=1}^{\infty} 2\pi i H_{\nu_l}^{(1)}(kr') \frac{e^{i\nu_l(2\pi+\theta)} + e^{i\nu_l(2\pi-\theta)}}{1 - e^{i\nu_l 2\pi}} \frac{H_{\nu_l}^{(2)}(ka)}{\frac{\partial}{\partial \nu} H_\nu^{(1)}(ka)|_{\nu=\nu_l}} H_{\nu_l}^{(1)}(kr)$$

(6.42)

where ν_l (with $l = 1, 2, 3, ...$) labels the zeros of the Hankel functions, $H_\nu^{(1)}(ka)$, in the upper complex ν-plane. Expression (6.42) is still exact. The semiclassical approximation is to evaluate the Hankel functions $H_\nu^{(1)}(ka)$ and $H_\nu^{(2)}(ka)$ under the Airy approximation (which is valid for $ka \gg 1$)

$$H_\nu^{(1)}(ka) \sim \frac{2}{\pi} e^{-i\frac{\pi}{3}} \left(\frac{6}{ka}\right)^{\frac{1}{3}} A(q^{(1)}) \qquad \text{and} \qquad H_\nu^{(2)}(ka) \sim \frac{2}{\pi} e^{+i\frac{\pi}{3}} \left(\frac{6}{ka}\right)^{\frac{1}{3}} A(q^{(2)})$$

with (see ref.[28])

$$q^{(1)} \equiv e^{-i\frac{\pi}{3}} \left(\frac{6}{ka}\right)^{\frac{1}{3}} (\nu - ka) \qquad \text{and} \qquad q^{(2)} \equiv e^{+i\frac{\pi}{3}} \left(\frac{6}{ka}\right)^{\frac{1}{3}} (\nu - ka).$$

Thus

$$\nu_l \quad \sim \quad ka + q_l \left(\frac{1}{6} ka\right)^{\frac{1}{3}} e^{i\frac{\pi}{3}} := ka(1 + i\alpha_l/k)$$

(6.43)

and

$$\nu_l \quad \simeq \quad ka \quad \text{for } ka \gg 1$$

(6.44)

where the q_ℓ's are the zeros of the Airy integral $A(q) = \int_0^\infty dt \cos(qt - t^3)$, approximately given by $q_l \approx \frac{1}{2}(6)^{\frac{1}{3}}(3\pi\{l - \frac{1}{4}\})^{\frac{2}{3}}$. The coefficients α_l are damping coefficients introduced in the Keller derivation above (6.5)

$$\alpha_l = q_l e^{-i\pi/6} \left(\frac{k}{6a^2}\right)^{\frac{1}{3}}, \qquad l = 1, 2, 3, \ldots.$$

(6.45)

This approximation is justified since there are two competing saddles in the integral representation of $H_\nu^{(1)}(ka)$ in the case $H_\nu^{(1)}(ka) = 0$ which is the condition for the poles. After inserting the Airy approximations into (6.42) and using

$$A(q_l^{(2)}) = \frac{\pi}{6} \frac{e^{-i\pi/6}}{A'(q_l^{(1)})}$$

(6.46)

which follows from the Wronskian of Airy integrals[1],

$$A(z)A'(ze^{\pm i2\pi/3}) - A'(z)A(ze^{\pm i2\pi/3}) = -\frac{\pi}{6} e^{\mp i\pi/6} ,$$

(6.47)

the energy-domain creeping propagator becomes

$$G_{\text{creep}}(k\vec{r}, k\vec{r}') \sim \sum_{l=1}^{\infty} \frac{1}{4i} H_{\nu_l}^{(1)}(kr') D_l \frac{e^{i\nu_l(2\pi+\theta)} + e^{i\nu_l(2\pi-\theta)}}{1 - e^{i\nu_l 2\pi}} D_l \frac{1}{4i} H_{\nu_l}^{(1)}(kr) ,$$

(6.48)

with

$$D_l = 2^{\frac{1}{3}} 3^{-\frac{2}{3}} \pi e^{i5\pi/12} \frac{(ka)^{\frac{1}{6}}}{A'(q_l^{(1)})} \; . \tag{6.49}$$

Finally we replace the remaining Hankel functions, $H_{\nu_l}^{(1)}(kr')$ and $H_{\nu_l}^{(1)}(kr)$, by their Debye approximation (6.35), a step which is justified, since we work under the condition that $|\vec{r}'| > |\vec{r}| \gg a \approx |\nu_l/k|$. The Debye approximation for the Hankel functions reads

$$H_{\nu_l}^{(1)}(kr) \sim \left(\frac{2}{\pi \sqrt{(kr)^2 - \nu_l^2}} \right)^{\frac{1}{2}} e^{i\sqrt{(kr)^2 - \nu_l^2} - i\nu_l \arccos(\nu_l/kr) - i\pi/4} \; . \tag{6.50}$$

We would of course like if we could substitute the disk radius a for the ratio ν_l/k since we would then obtain the creeping ray interpretation of *all* the l-mode contributions. In order to check if this is a valid approximation we write the zeros of the Hankel functions in the Airy approximation as

$$\nu_l = ka(1 + i\alpha_l/k) := ka + \delta\nu_l = ka \left(1 + \mathcal{O}(\hbar^{\frac{2}{3}}) \right) \tag{6.51}$$

Inserting this into the Debye approximation and expanding to the second order in $\delta\nu_l$ we obtain

$$
\begin{aligned}
\sqrt{k^2 r^2 - \nu_l^2} - \nu_l \arccos(\nu_l/kr) &= k\sqrt{r^2 - a^2} - ka \arccos(a/r) - \delta\nu_l \arccos(a/r) \\
&\quad + \frac{1}{2} \frac{(\delta\nu_l)^2}{k\sqrt{r^2 - a^2}} + \mathcal{O}(\delta\nu_l^3) \\
&= k\sqrt{r^2 - a^2} - \nu_l \arccos(a/r) + \frac{1}{2} \frac{(\delta\nu_l)^2}{k\sqrt{r^2 - a^2}} + \mathcal{O}(\delta\nu_l^3) \\
&= k\sqrt{r^2 - a^2} - \nu_l \arccos(a/r) + \mathcal{O}(\hbar^{\frac{1}{3}}) \\
&= \frac{1}{\hbar} \left(p\sqrt{r^2 - a^2} - \hbar\nu_l \arccos(a/r) + \mathcal{O}(\hbar^{\frac{4}{3}}) \right) \tag{6.52}
\end{aligned}
$$

for the exponent, where we have used the relation $p = \hbar k$. In this calculation the linear terms arising from the square root and from the arc cosine cancels exactly allowing us to obtain the creeping interpretation of the geometrical contents of the expression. For the prefactor a similar calculation gives

$$
\begin{aligned}
\frac{1}{(k^2 r^2 - \nu_l^2)^{\frac{1}{4}}} &= \frac{1}{(k\sqrt{r^2 - a^2})^{\frac{1}{2}}} + \frac{1}{2} \frac{ka\delta\nu_l}{(k\sqrt{r^2 - a^2})^{\frac{5}{2}}} + \mathcal{O}(\frac{(\delta\nu_l)^2}{(k\sqrt{r^2 - a^2})^{\frac{5}{2}}}) \\
&= \frac{1}{(k\sqrt{r^2 - a^2})^{\frac{1}{2}}} \left(1 + \frac{1}{2} \frac{ka\,\delta\nu_l}{(k^2(r^2 - a^2))} + \mathcal{O}(\hbar^{\frac{4}{3}}) \right) \\
&= \frac{1}{(k\sqrt{r^2 - a^2})^{\frac{1}{2}}} \left(1 + \mathcal{O}(\hbar^{\frac{2}{3}}) \right) \tag{6.53}
\end{aligned}
$$

Note, it is not justified to throw away the $\delta\nu_l \arccos(a/r)$ term in the exponent, since this term scales as $\mathcal{O}(\hbar^{-\frac{1}{3}})$. The $\mathcal{O}(\hbar^{\frac{2}{3}})$ correction of the prefactor can

however be safely neglected, since it is a $\mathcal{O}(\hbar)$ correction to the above mentioned term in the exponent.

Inserting these expansions into (6.48) we get modulo $\mathcal{O}(\hbar^{\frac{2}{3}})$ corrections in the semiclassical limit

$$
\begin{aligned}
G_{\text{creep}}(k\vec{r}, k\vec{r}') \quad \sim \quad & \frac{1}{4i}\left(\frac{2}{\pi k\sqrt{r'^2 - a^2}}\right)^{\frac{1}{2}} e^{ik\sqrt{r'^2 - a^2} - i\pi/4} \\
& \times \sum_{l=1}^{\infty} D_l \, \frac{e^{i\nu_l\{2\pi + \theta - \arccos(a/r') - \arccos(a/r)\}} + e^{i\nu_l\{2\pi - \theta - \arccos(a/r') - \arccos(a/r)\}}}{1 - e^{i\nu_l 2\pi}} \, D_l \\
& \times \frac{1}{4i}\left(\frac{2}{\pi k\sqrt{r^2 - a^2}}\right)^{\frac{1}{2}} e^{ik\sqrt{r^2 - a^2} - i\pi/4}
\end{aligned}
$$

$$(6.54)$$

Comparing this expression to (6.18) we see that they coincide and thus that the diffraction coefficients D_l in (6.54) are to be identified with the original introduced diffraction coefficients D_m in (6.4). By using the Airy approximation of the ν_l's (6.43) we also note that the phase factors $e^{i\nu_l\theta_{diff}}$ contains a damping term of the form $\exp(-\theta_{diff}q_l(\frac{1}{6}ka)^{1/3}\sin(\pi/3))$, even when k is real. This is the damping exponential of the creeping path. This concludes our semiclassical evaluation of the 1-disk Greens function.

It should at this point be noted that the derivation above is not valid for rays that are almost grazing (tangent) or for rays that are scattered in a very forward direction. This is due to that in the illuminated region the Debye approximation fails if $(ka - l_r) \leq (ka)^{1/3}$, where l_r is the angular momentum of the reflected ray. In the shadow region the residuum resumation fails if the creeping angle becomes very small i.e. of order $\alpha \leq (ka)^{1/3}$. The region in between the illuminated and the shadow region is called the *penumbra* and if one wants to evaluate the Greens function here one should consider the *penumbra corrections* as introduced by Smilansky et. al [43] and which are different from the creeping contributions discussed above. In the examples we are going to study which are basically the three-disk scattering system, the periodic orbits are composed by segments that are either purely geometric or purely creeping since the ray wind around the disk by at least $\pi/3$. We shall therefore not consider these contributions further.

6.3.3   Fields diffracted by edges

As a further development of the geometrical theory of diffraction in two dimensions we here consider the field diffracted by the sharp edge or vertex of two semi infinite straight lines meeting with an angle $(2 - n)\pi$, where $0 \leq n \leq 2$ is a real number [54, 39]. We proceed in quite the same fashion as in the case of diffraction by a smooth object and start by introducing the usual polar coordinate system (ρ, θ) with the vertex of the wedge centered at the origin of the coordinate system. We let α and θ be the angles of the incident and diffracted

rays measured with respect to the direction normal to the wedge on the side
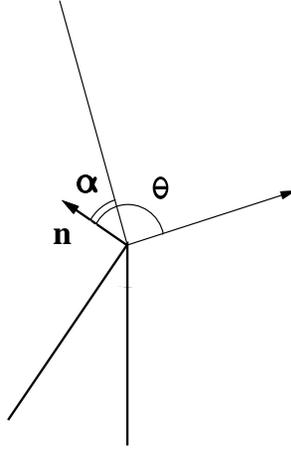where the rays come from (see figure 6.5).

Figure 6.5: The geometry of the incident and diffracted rays, and the wedge.

First of all the free propagation is still done by the usual geometrical optics
so that the field is described by rays that are straight lines (in a homogeneous
medium) and the field at distance R from a source of unit strength is given
by (6.15). To find the amplitude $A(r)$ we consider the tube enclosed by two
neighbouring rays. The cross-sectional area of this tube is proportional to r and
the flux through it is proportional to rA^2. As a consequence of flux conservation
we therefore find that $A(r)$ must be proportional to $r^{-1/2}$. As in the case of
diffraction by a smooth object we also assume that the diffracted amplitude is
proportional to the incident amplitude and we can therefore write

$$u_d = Du_i r^{-1/2} e^{ikr} \tag{6.55}$$

where u_i denotes the incident field, and D is the diffraction constant. As in
the case of the 1-disk system we can, because of the simple structure of the
problem, obtain an exact solution for the Greens function also in this case.
This is done in detail in ref.[67, 68]. Here we merely state the result of this
asymptotic expansion which reads

$$
\begin{aligned}
u_d \simeq & \; \frac{e^{ikr}}{\sqrt{kr}} \\
\times & \; \frac{\sin(\pi/n)}{n}[(\cos(\pi/n) - \cos((\theta - \alpha)/n)^{-1} - (\cos(\pi/n) - \cos((\theta + \alpha + \pi)/n)^{-1}]
\end{aligned}
$$

Comparison to equation (6.55) now yields

$$D = \frac{\sin(\pi/n)}{n}[(\cos(\pi/n) - \cos((\theta - \alpha)/n)^{-1} - (\cos(\pi/n) - \cos((\theta + \alpha + \pi)/n)^{-1}]$$

which is the expression for the diffraction constant in case of edge diffraction.

6.4   The general Keller propagator

We next adress the problem of getting the complete Greens function in the general case. Here there might be many different obstacles and therefore many different trajectories leading from the source to the receiver. For each such ray ξ the contribution to the Green's function is the product of the Green's functions and diffraction coefficients along the ray:

$$
\begin{aligned}
G_\xi(q_\mathcal{A}, q_\mathcal{B}, E) \quad = \quad & \prod_{i=1}^{n_\xi} G_i(q_\mathcal{A}, q_{\mathcal{A}'}, E) \sum_{l=1}^{\infty} D_{l,\mathcal{A}'} G_l^D(q_{\mathcal{A}'}, q_{\mathcal{B}'}, E) \\
& \times D_{l,\mathcal{B}'} G(q_{\mathcal{B}'}, q_\mathcal{B}, E).
\end{aligned}
\tag{6.56}
$$

where n_ξ is the number of segments of the path and the Greens functions are either the Van Vleck, the creeping or the edge diffraction propagators. To get the complete Greens function $G(q, q', E)$ of the system we should then finaly sum up the contributions of the form (6.56) for *all* the paths that connects q with q' at energy E

$$
G(q, q', E) \quad = \quad \sum_{\xi : q \to q'} G_\xi(q, q')
\tag{6.57}
$$

where ξ labels the paths connecting q with q' at energy E.

6.4.1   Connection to the trace formula

To incorporate diffraction effects into the trace formula, one should compute the trace of the Green's function derived above. As in the case of the Gutzwiller trace formula – derived from a pure geometrical approximation of the Green's function – the trace receives the leading contributions from tubes encircling the closed curves, which now can have diffractional arcs too. In the case of ordinary geometrical orbits the trace can be evaluated in terms of a saddlepoint approximation which transforms the integral to a sum over paths that are not just closed but are in fact periodic. This is due to the fact that the saddle point condition is equivalent to identifying initial and final momentum. In the case of creeping orbits, the situation is not that straightforward since we are dealing with hard wall potentials that does not allow for variation of the path on the inside of the boundary of the obstacle. This means that we can only approach the saddle point from one side which inhibits the usual saddle point approximation. At this point it is therefore not clear how to proceed with the usual scheme to obtain the trace. Since the aim of all our efforts is not directly to get the trace but to obtain a quantization condition i.e. a condition for a complex k value to be a resonance of the system we shall here take another approach to this problem than the usual direct trace integration. We simply determine the exact quantum mechanical resonance condition for a simple example (the two-disk scattering system) and then make the usual cycle expansion ansatz for the spectral determinant related to the scattering problem. By comparison of the exact resonance condition and the cycle expansion we then can obtain a

rule relating the ingredients of the semiclassical propagator including diffraction terms to the weigths of the periodic orbits used in the cycle expansion. That this procedure is valid and really gives an approximation to the exact quantum mechanical resonances, were recently shown by A. Wirzba and M. Henseler [66]. In a remarkable work they investigate the two-dimensional scattering of a point particle from n non-overlapping fixed disks and study the connection between the spectral properties of the quantum mechanical scattering matrix and its semi-classical equivalent based on the Gutzwiller-Voros zeta function. They rewrite the determinant of the scattering matrix in such a way that it separates into a product over n determinants of 1-disk scattering matrices (representing the incoherent part of the scattering from the n-disk system) and the ratio of two mutually complex conjugate determinants of the genuinely multi-disk scattering kernel $\mathbf{M}$, which represents the coherent part of the scattering

$$\det \mathbf{S}^{(n)}(k) = \left\{ \prod_{j=1}^{n} \det \mathbf{S}^{(1)}(ka_j) \right\} \frac{\det \mathbf{M}(k^*)^{\dagger}}{\det \mathbf{M}(k)} \tag{6.58}$$

where a_j are the radii of the n disks. Further more they show that in the semi-classical limit, the $\mathbf{M}$ determinants will approach the Gutzwiller-Voros spectral determinants *with the inclusion of diffractional periodic orbits*. In the following we shall sketch how this relation can be obtained just for the $\mathbf{M}$ determinant which is sufficient to obtain the scattering resonances i.e. the poles of the scattering matrix $\mathbf{S}$.

6.4.2 The exact poles of the scattering matrix

As a specific example we choose the two disk scattering system which has only a single geometric periodic orbit. We shall here mainly follow A. Wirzba [60, 61] and Gaspard and Rice [32]. In [32] it was found that the Scattering matrix $\mathbf{S}$ had the following structure

$$\mathbf{S} = \mathbf{1} - i\mathbf{C}\mathbf{M}^{-1}\mathbf{D} \tag{6.59}$$

The exact quantum mechanical resonances are found as the pole of the scattering matrix which then becomes the wave numbers where the characteristic determinant $\det \mathbf{M}(k)$ vanishes

$$\det \mathbf{M}(k) = 0. \tag{6.60}$$

The matrix $\mathbf{M}$ can be constructed according to the methods in ref.[32], and for the A_1 symmetry (which corresponds to regarding the fundamental domaine as the system in it self) it has the following structure

$$\mathbf{M} = \mathbf{1} + \mathbf{A}$$
$$\mathbf{A}_{mm'} = \frac{1}{2} \frac{J_m(ka)}{H_{m'}^{(1)}(ka)} \left((-1)^{m'} H_{m-m'}^{(1)}(kR) + H_{m+m'}^{(1)}(kr) \right). \tag{6.61}$$

Here R is the seperation of the centers of the two disks wheras a is the radius of the disks. Since $\mathbf{M}(k)$ has the structure $\mathbf{M}(k) = \mathbf{1} + \mathbf{A}(k)$, it is natural to

expand the determinant in the characteristic equation (6.60) as

$$
\begin{aligned}
\det \mathbf{M} &= \exp(\mathrm{Tr}\ln(\mathbf{1} + \mathbf{A})) \\
&= 1 + \mathrm{Tr}\mathbf{A} - \frac{1}{2}[\mathrm{Tr}\mathbf{A}^2 - (\mathrm{Tr}\mathbf{A})^2] + \ldots
\end{aligned}
\tag{6.62}
$$

This procedure is mathematically valid since the matrix $\mathbf{A}$ is *trace class* [66]. We now make the ansatz that (6.62) should be semiclassicaly represented by some Gutzwiller-Voros like spectral determinant

$$
\tilde{Z}(z, k) = \prod_p \prod_{l=0}^{\infty} (1 - t_{p_l}(k) z^{n_p})
\tag{6.63}
$$

where the prime periodic orbits should now allow also for diffractive periodic orbits. In (6.63) z is as usual just a book keeping parameter keeping track of the topological order n_p of the cycles. In the end after expanding the determinant in powers of z it will finally be put equal to 1. To get the ansatz into a shape where it is comparable to (6.62) we rewrite it as

$$
\begin{aligned}
\tilde{Z}(z, k) &= \exp\left(\sum_p \sum_{l=0}^{\infty} \ln(1 - t_{p_l}(k) z^{n_p}) \right) \\
&= \exp\left(-\sum_p \sum_{l=0}^{\infty} \sum_{m=1}^{\infty} \frac{(t_{p_l}(k) z^{n_p})^m}{m} \right) \\
&\equiv \exp\left(-\sum_{n=1}^{\infty} \mathrm{Tr}_n z^n \right)
\end{aligned}
\tag{6.64}
$$

where we have gathered all terms of power z^n in the terms Tr_n. Expanding the exponential this finally yields

$$
\tilde{Z}(z, k) = 1 - \mathrm{Tr}_1 z - \frac{1}{2}(\mathrm{Tr}_2 - \mathrm{Tr}_1^2) z^2 + \ldots
\tag{6.65}
$$

As we see this has exactly the same structure as (6.62) due to the expansion of an exp(log) in both cases. It is therefore natural to make the transition from exact quantum mechanics to semiclassics at this point since this yields a shortcut compared to the trace evaluation of the creeping Greens function.

To proceed we then have to first get $\mathbf{A}$ and evaluate its trace and then compare this to our semiclassical ingredients from the geometrical and creeping propagators.

For the A_1 subspace the matrix $\mathbf{A}$ is [60]

$$
\mathbf{A}_{m,m'} = \frac{1}{2} \frac{J_m(ka)}{H_{m'}^{(1)}(ka)} \left((-1)^{m'} H_{m-m'}^{(1)}(kR) + H_{m+m'}^{(1)}(kR) \right)
\tag{6.66}
$$

which gives the trace

$$
\mathrm{Tr}\mathbf{A} = \frac{1}{2} \sum_{m=-\infty}^{+\infty} \frac{J_m(ka)}{H_m^{(1)}(ka)} \left((-1)^{m'} H_0^{(1)}(kR) + H_{2m}^{(1)}(kR) \right).
\tag{6.67}
$$

Using the Watson transformation (6.25) we can transform the sum to a complex contour integral

$$\text{Tr}\mathbf{A} \quad = \quad \frac{1}{4i} \oint_C d\nu \frac{1}{\sin(\pi\nu)} \frac{J_\nu(ka)}{H_\nu^{(1)}(ka)} \left(H_0^{(1)}(kR) + \exp(-i\nu\pi) H_{-2\nu}^{(1)}(kR) \right),$$

where we used $H_{-2m}^{(1)}(kr) = H_{2m}^{(1)}(kr)$. As in the case of the one disk propagator we can transform the contour path C to run in the upper half plane by substituting $-\nu$ for ν in the second part of the contour integral

$$\frac{1}{4i} \oint_C d\nu \ldots \quad = \quad \frac{1}{4i} \int_{+\infty+i\epsilon}^{-\infty+i\epsilon} d\nu \ldots \frac{1}{4i} \int_{-\infty-i\epsilon}^{+\infty-i\epsilon} d\nu \ldots . \tag{6.68}$$

After some rewriting where we use for instance [1]

$$H_{-\nu}^{(1)}(kr) \quad = \quad \exp(i\nu\pi) H_\nu^{(1)}(kr)$$

and

$$J_{-\nu}(kr) \quad = \quad \frac{1}{2} \left(\exp(i\nu\pi) H_\nu^{(1)}(kr) + \exp(-i\nu\pi) H_\nu^{(1)}(kr) \right) \tag{6.69}$$

the trace reads

$$\text{Tr}\mathbf{A} \quad = \quad \frac{1}{4} \int_{-\infty+i\epsilon}^{+\infty+i\epsilon} d\nu \frac{H_\nu^{(2)}(ka)}{H_\nu^{(1)}(ka)} \left(\exp(-i\nu\pi) H_0^{(1)}(kR) + \exp(-2i\nu\pi) H_{-2\nu}^{(1)}(kR) \right)$$

$$- \frac{1}{2i} \int_{-\infty+i\epsilon}^{+\infty+i\epsilon} d\nu \frac{H_\nu^{(2)}(ka)}{H_\nu^{(1)}(ka)} \left(\frac{1}{\sin(\nu\pi)} H_0^{(1)}(kR) + \frac{\exp(-i\nu\pi)}{\sin(\nu\pi)} H_{-2\nu}^{(1)}(kR) \right)$$

As in the case of the 1-disk propagator we can here split the trace into a geometrical and a creeping contribution, where the latter is the one that still contains the Watson denominator $\sin(\nu\pi)$. Under the semiclassical assumption that $ka >> 1$ we can therefore evaluate the integral by using the same procedure as in the case of the 1-disk Greens function. The geometrical part of the trace yields [61]

$$\text{Tr}\mathbf{A}_{geo} \quad \simeq \quad \frac{1}{2} \sqrt{\frac{a}{2R}} \left(1 + \frac{1}{\sqrt{1-2a/R}} \right) \exp(ik(R-2a)) \tag{6.70}$$

Truncating the cumulant expansion (6.62) to the first order in $\mathbf{A}$ we therefore get the condition for resonances using only geometrical input

$$1 - \frac{1}{2} \sqrt{\frac{a}{2R}} \left(1 + \frac{1}{\sqrt{1-2a/R}} \right) \exp(ik(R-2a)) \quad = \quad 0 \tag{6.71}$$

This should be compared to the first order truncation of the cycle expansion of the semiclassical expression for the spectral determinant i.e. the Gutzwiller-Voros determinant

$$\Delta_G(k) \quad = \quad \prod_{l=0}^{\infty} \left(1 - \frac{e^{ikT_0} z}{\Lambda_0^{(1+4l)/2}} \right)$$

$$\simeq \quad 1 - \frac{e^{ikT_0}}{\sqrt{\Lambda_0}(1-\Lambda_0^{-2})} \tag{6.72}$$

where the fact that the stability is squared comes from the symmetry reduction since we are dealing with a boundary orbit. From the analytic expression for Λ_0

$$\Lambda_0 \;\; = \;\; \frac{R - a + \sqrt{R^2 - 2Ra}}{a} \tag{6.73}$$

it can indeed be shown that (see appendix 9.2):

$$\frac{1}{2}\sqrt{\frac{a}{2R}}\left(1 + \frac{1}{\sqrt{1 - 2a/R}}\right) \;\; = \;\; \frac{1}{\sqrt{\Lambda_0}(1 - \Lambda_0^{-2})} \tag{6.74}$$

so that the stability factor as well as the phase of the semiclassical expansion of the geometrical part are in comlete agreement with the ordinary semiclassical Gutzwiller-Voros expression of the spectral determinant.

The semiclassical evaluation of the creeping part of Tr$\mathbf{A}$ takes place in exactly the same fashion as in the 1-disk propagator. There are two fundamental creeping paths corresponding to the two kR-dependant Hankel functions $H_0^{(1)}(kR)$ and $H_{-2\nu}^{(1)}(kR)$. Following [60, 28] we can therefore immediately write down the contributions

$$\begin{aligned}
\mathrm{Tr}\mathbf{A}_{creepa} \;\; &\simeq \;\; -\sqrt{\frac{a}{2R}}\frac{\exp(i\pi/12)}{(ka)^{1/6}}\exp(ikR)\sum_{l=1}^{\infty}C_l\frac{\exp(i\nu_l\pi)}{1 - \exp(2i\nu_l\pi)}\\
&= \;\; \frac{1}{4i}\sqrt{\frac{2}{\pi kR}}e^{ikR - i\pi/4}\sum_{l=1}^{\infty}D_l^2\frac{e^{i\nu_l\pi}}{1 - \exp(i\nu_l 2\pi)}
\end{aligned} \tag{6.75}$$

where we used the expression (6.49) for D_l in order to make the expression resemble the creeping propagator (6.54), and where

$$C_l \;\; = \;\; \frac{1}{3}\frac{\pi^{3/2}}{6^{1/3}}\frac{1}{A'(q_l)^2} \tag{6.76}$$

whith $A'(q_l)$ denoting the derivative of the Airy integral at q_l. In the expression (6.75) we recognize the exact form of the creeping propagator for the '0' shaped orbit in the fundamental domain.

The b trace yields similarly

$$\begin{aligned}
\mathrm{Tr}\mathbf{A}_{creepb} \;\; &\simeq \;\; -\sqrt{\frac{a}{2R}}\frac{\exp(i\pi/12)}{(ka)^{1/6}}\sum_{l=1}^{\infty}C_l\left(\frac{k^2R^2}{k^2R^2 - 4\nu_l^2}\right)^{1/4}\\
&\times \;\; \exp\left(i\sqrt{k^2R^2 - 4\nu_l^2}\frac{\exp[i\nu_l(\pi + 2\arcsin(2\nu_l/kR))]}{1 - \exp(2i\nu_l\pi)}\right)\\
&= \;\; \frac{1}{4i}\sum_{l=1}^{\infty}\left(\frac{2}{\pi k\sqrt{R^2 - 4\nu_l^2}}\right)^{1/2}e^{ik\sqrt{R^2 - 4\nu_l^2} - i\pi/4}D_l^2\frac{e^{i\nu_l(2\pi - 2\cos^{-1}(2\nu_l/kR))}}{1 - e^{i\nu_l 2\pi}}\\
&\simeq \;\; \frac{1}{4i}\left(\frac{2}{\pi k\sqrt{R^2 - 4a^2}}\right)^{1/2}e^{ik\sqrt{R^2 - 4a^2} - i\pi/4}\sum_{l=1}^{\infty}D_l^2\frac{e^{i\nu_l(2\pi - 2\cos^{-1}(2a/R))}}{1 - e^{i\nu_l 2\pi}}
\end{aligned}$$

where we used the approximation

$$\nu_l \simeq ka \tag{6.77}$$

which is valid for large values of ka. In both cases the sum runs over the zeros ν_l of the Hankel function $H_\nu^{(1)}(ka)$ in the upper half plane. In the last expression we recognize the contribution to the Greens function from the periodic ∞ shaped orbit in the fundamental domaine.

By comparison to the cumulant expansion it then becomes clear how to get the resonance condition at least to the first order: to get the trace of $\mathbf{A}$, we simply take the contributions to the Greens function from all the periodic orbits of topological length 1 including the *diffractive* orbits. For the higher orders in z terms like $(\text{Tr}\mathbf{A})^2$ gives combinations of shorter orbits whereas $\text{Tr}\mathbf{A}^n$ terms will contain higher order periodic creeping orbits. That this is so for the two disk system is quite obvious because of the simple geometry. For a general N-disk system the proof is not quite that simple but for low orders in z it can be checked by direct computation of the traces. In the three disk system the relation between low order periodic creeping orbits and the trace of $\mathbf{A}$ has been performed by A. Wirzba [60, 61].

Even though it is not necessary for finding the resonances we can now also get the semiclassical approximation of the trace by using the relation

$$\text{Tr}G(E) \ = \ \frac{d}{dE}\ln\Delta(E) \tag{6.78}$$

Here the diffraction as well as the creeping segments will give extra contributions compared to the usual geometrical time contribution, but since these contributions are of the order $(ka)^{-2/3}$ we can neglect these since we have already done this in our approximation of ν_l. The diffraction contribution to the trace therefore reads in this approximation

$$\text{Tr}G_D(E) \ = \ \sum_{cycles}\frac{T(E)}{i\hbar}\prod_{i=1}^{n}D(q_i)G(q_i,q_{i+1},E) \tag{6.79}$$

where $T(E)$ is the time period of the cycle (without repeats) and $G(q_i,q_{i+1},E)$ is alternatingly the free propagator and the creeping propagator.

6.4.3 Cycle expansion of the diffraction spectral determinant

To apply the diffraction spectral determinant we here discuss how to use the well known cycle expansion [18] to calculate this. Using the ansatz (6.63) the total spectral determinant can be written

$$\Delta(k) \ = \ \Delta_G(k)\Delta_D(k) \tag{6.80}$$

where we have split the formal product into the usual Gutzwiller Voros spectral determinant representing the purely geometrical input and the diffractive

spectral determinant representing the new information obtained from the geometrical theory of diffraction. The product is only formal, since the eigenenergies are not given by the zeros of $\Delta_G(E)$ or $\Delta_D(E)$ individually, but have to be calculated from a curvature expansion of the *combined* determinant $\Delta(E)$ itself.

The diffraction part of the spectral determinant is

$$\Delta_D(E) = \exp\left(-\sum_{p,r=1}^{\infty} \frac{1}{r} \prod_{i=1}^{n_p} [D(q_i^p)G(q_i^p, q_{i+1}^p, E)]^r\right), \tag{6.81}$$

where the summation goes over closed primitive (non-repeating) cycles p and the repetition number r. The product of Green's functions should be evaluated for q_i^p belonging to the primitive cycle p. After summation over r, the spectral determinant can be written as

$$\Delta_D(E) = \prod_p (1 - t_p) \tag{6.82}$$

with

$$t_p = \prod_{i=1}^{n_p} D(q_i^p)G(q_i^p, q_{i+1}^p, E), \tag{6.83}$$

where q_i^p belongs to the primitive cycle p. Here the mode numbers l of the diffraction constants and the corresponding summations have been surpressed for notational simplicity; they can be easily restored as e.g. in the final expression (6.92).

We can conclude that the diffractional part $\Delta_D(E)$ of the spectral determinant shares some nice features of the periodic orbit expansion of the dynamical zeta functions[18], and it can be expanded as

$$\Delta_D(E) = 1 - \sum_p t_p + \sum_{p,p'} t_p t_{p'} - \cdots . \tag{6.84}$$

Now if we restrict ourselves to include only the $l = 1$ mode then the weight (6.83) has the following property which helps in radically reducing the number of relevant contributions in the expansion: If two different cycles p and p' have at least one common piece in their diffraction arcs, then the two cycles can be composed to one longer cycle $p + p'$ and the weight corresponding to this longer cycle is the product of the weights of the short cycles

$$t_{p+p'} = t_p \cdot t_{p'}. \tag{6.85}$$

As a consequence, the product of primitive cycles, which have at least one common piece in their diffraction arcs, can be reduced in such a way that the composite cycles are exactly canceled in the curvature expansion

$$\prod_p (1 - t_p) = 1 - \sum_b t_b, \tag{6.86}$$

where t_b are *basic* primitive orbits which can not be composed from shorter primitive orbits. To see that this nice composition rule does not hold if we include the higher l modes as well, we can consider the two shortest pure creeping orbits and their composition in the two-disk system. These two orbits are then the 0- and the ∞ shaped orbits. If we consider the two orbits in the fundamental domain, they will have the following schematic form

$$\begin{aligned}
t_0 &= \frac{e^{ikR}}{\sqrt{R}} \sum_l C_l e^{i\nu_l \pi} \\
t_\infty &= \frac{e^{ik\sqrt{R^2 - 4a^2}}}{\sqrt{(R^2 - 4a^2)^{1/2}}} \sum_l C_l e^{i\nu_l \pi + i\nu_l 2\theta}
\end{aligned} \tag{6.87}$$

where θ is the little extra angle the ray has to creep in the case of the ∞ shaped orbit as compared to the 0 shaped orbit. The above weights are only given modulus an for this purpose unimportant overall factor. The composition of the two orbits can be constructed by first following the 0- and then the ∞ shaped orbit. The weight for the composed orbit therefore reads

$$\begin{aligned}
t_{0\infty} &= \frac{e^{ikR}}{\sqrt{R}} \sum_l C_l e^{i\nu_l \pi + i\nu_l \theta} \frac{e^{ik\sqrt{R^2 - 4a^2}}}{\sqrt{(R^2 - 4a^2)^{1/2}}} \sum_{l'} C'_l e^{i\nu'_l \pi + i\nu'_l \theta} \\
&= const \times \sum_{ll'} C_l C_{l'} e^{i(\nu_l + \nu_{l'})\pi + i(\nu_l + \nu_{l'})\theta}
\end{aligned} \tag{6.88}$$

If the composition rule were to hold when including all the l modes we would expect that the expression (6.88) should be the product of the two individual terms in (6.87). By taking the product

$$t_0 t_\infty = const \times \sum_{ll'} e^{i(\nu_l + \nu_{l'})\pi + i2\nu_{l'}\theta} \tag{6.89}$$

we see that this is not the case in general. This is due to that in the composed orbit the overlapping creeping segments are not identical to any of the original creeping segments, since the orbit shifts from "0"-creeping to "∞"-creeping each time the ray creeps around the disk. Of course the composition rule would still hold if the creeping segments were identically the same, as it is the case for repetitions of a creeping orbit: $t_{2a} = t_a^2$.

6.5   Numerical results

In this section we try to demonstrate the significance of the diffraction corrections to the trace formula. As working examples we have chosen our usual

favorite systems: the two- and three-disk scattering systems. In order to be able to use only the basic primitive orbits and the composition rule for these, we have restricted the calculations to the $l = $ mode only. As the real part of the damping coefficient α_l goes like $\alpha_l(k) = const \times \text{Re } k^{1/3}(l - \frac{1}{4})^{2/3}$, and since the diffraction coefficients C_l is a decreasing function of l, we assume that the calculation will give the leading behaviour of the full spectral determinant.

6.5.1   Results for the two-disk system

To demonstrate the importance of the diffraction effects to the spectra, we have calculated the A_1 resonances of the scattering system of two equally sized hard circular disks with disk separation $R = 6a$, where a is the radius of one disk. In this system there is only one geometrical periodic cycle along the line connecting the centers of the disks. Its stability $\Lambda_p = 9.8989794$ and action $S_p = kL_p = k \cdot 4a$, yield the geometrical part of the spectral determinant[16, 61]

$$\Delta_G(k) = \prod_{j=0}^{\infty} \left(1 + \frac{e^{ikL_p}}{\Lambda_p^{(1+4j)/2}} \right), \tag{6.90}$$

where $k = \sqrt{2mE}/\hbar$ and $2m = \hbar = 1$, and leads to the following predictions for the semiclassical A_1 resonances

$$k_{n,j}^{\text{res}} = \left(\pi(2n - 1) - i\frac{1 + 4j}{2} \ln \Lambda_p \right) / L_p \tag{6.91}$$

with $n = 1, 2, 3, \cdots$. Note in the above expressions $(1 + 4j)/2$ replaces the usual weight $(1 + 2j)/2$, since the geometrical orbit in the two-disk problem lies on the boundary of the fundamental domain.

Fig. 6.6 shows the first four new basic cycles in the fundamental domain[16]. We computed the geometrical data of the first ten orbits and used them to construct the creeping and geometrical Green's functions. If the ray connecting q and q' is reflected once or more from the curved hard walls before hitting tangentially one of the surfaces, we can keep track of the change in the amplitude by the help of the Sinai-Bunimovich curvatures (6.41). The effective radius R_b^{eff}, the length of the geometrical arc L_b^G and the length of the diffraction part L_b^D of the first ten orbits with creeping sections are listed in Table 6.1.

The diffraction part of the spectral determinant is finally given by

$$\Delta_D(k) = 1 - \sum_{b,l} (-1)^{m_b} C_l \frac{a^{1/3} e^{i\pi/12} e^{ik(L_b^G + L_b^D) - \alpha_l L_b^D}}{k^{1/6}\sqrt{R_b^{\text{eff}}}}$$

$$\times \frac{1}{1 - e^{2\pi(ik - \alpha_l)a}}, \tag{6.92}$$

where $C_l = \pi^{3/2} 3^{-4/3} 2^{-5/6}/Ai'(x_l)^2$, and $Ai'(x_l)$ is the derivative of the Airy function evaluated at it's l'th zero x_l. We computed the spectra by truncating

m_b	L_b^G/a	R_b^{eff}/a	L_b^D/a
0	5.656854249492	5.656854249424	3.821266472498
0	6.000000000000	6.000000000000	3.141592653589
1	9.832159566199	58.16784043380	3.476488812029
1	9.797958971132	58.78775382679	3.544308495170
2	13.81654759452	578.1406653460	3.507404058891
2	13.81309379078	579.7434283719	3.514253447057
3	17.81499162871	5729.649817456	3.510488616089
3	17.81464272590	5732.235502463	3.511180541615
4	21.81483475355	56728.70010470	3.510799703655
4	21.81479950722	56732.26871144	3.510869602322

Table 6.1: The first ten basic cycles t_b which include creeping sections in the fundamental region of two-disk problem (with disk separation $R = 6a$). The cycles are labeled by the number m_b of geometrical reflections from one of the disks. The length of the geometrical arc L_b^G, the effective radius R_b^{eff} and the length of the diffraction segment L_b^D are listed in units of the disk radius a.

the product $\Delta_G(k)\Delta_D(k)$ at maximal cycle length 5 and using only the $l = 1$ term in the now restored summation over the creeping mode number. The exact quantum mechanical resonances were computed following ref.[60].

The leading semiclassical resonances are given equally well with and without creeping modifications. In fig. 6.7 we can see that the new formula describes the resonances of the two disk system with a few-percent error, while the computation based on the geometrical cycle alone, (6.90), gives completely false results for the next-to-leading resonances (see (6.91)).

6.5.2   Results for the 3-disk scattering system

In order to apply the geometrical theory of diffraction to the calculation of semiclassical resonances, we also have to account for the diffraction (creeping) orbits of the system. To give an overview of the work to be done, we start by counting the number of periodic creeping orbits to be evaluated. Because of the symmetry of the system we can assume that the creeping orbit always starts tangentially from the (half-) disk in the fundamental domain which we label disk number 1 see fig. 6.8. Considering first an orbit with no geometrical bounces we see that it has two different disks to go to, and for each each disk two different sides to creep in. This makes a total of four diffraction orbits of topological length 1. When these are folded back into the fundamental domain we see that two of them are self retracing. The two other orbits are tracing the same orbit, but in opposite directions. If we consider paths of the particle with m bounces, we see that there will be $2^{n+1} = 2^{m+2}$ periodic creeping orbits of topological order n, as for each one of the m bounces the particle can choose between two disks. Thus the number of periodic creeping orbits grows exponentially fast with
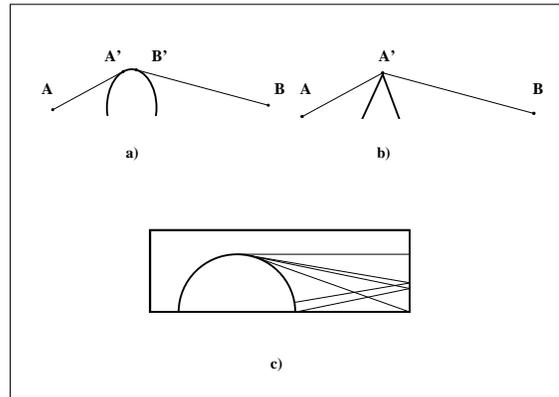
Figure 6.6: The simplest classes $\mathcal{D}_{100}$ (a) and $\mathcal{D}_{001}$ (b) of curves in two dimensions. In the window (c): the first four basic orbits in the fundamental domain of the two-disk system.
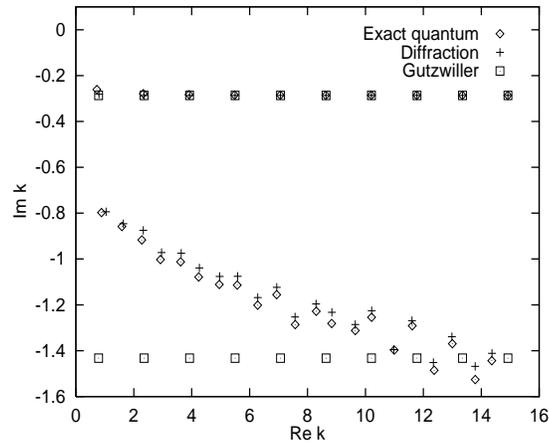

Figure 6.7: Resonances for the $A1$ subspace of the two-disk system (with disk separation $R = 6a$) in the complex k plane in units of the disk radius a. The diamonds label the exact quantum mechanical resonances, which are the poles of the scattering matrix. The crosses are their semiclassical approximations including the diffraction terms derived in this paper. The boxes refer to the ordinary Gutzwiller semiclassical approximation, with $(j = 0, 1)$, where the diffraction effects are not included.

the topological length, n, of the orbit. It is quite astonishing however, as we will see later, how few of these orbits are in fact needed to get a good description of the scattering resonances (including the ones with large imaginary parts). The creeping orbits can be described completely by their itinerary $1\alpha_1\alpha_2\ldots\alpha_n$ where the α_i's are taken from the alphabet $\{1, 2, 3\}$ and where we do not allow the repeats $\ldots 11\ldots$, $\ldots 22\ldots$ and $\ldots 33\ldots$. This description contains a double degeneracy due to the fact that the orbit has the choice to creep around the final disk clockwise or anti-clockwise. For instance, '123' can represent two different orbits which start from disk 1 in the fundamental domain, then hit disk number 2 and finally creep around the final disk (3) clockwise or anti-clockwise.

The restriction that the creeping periodic orbits should start and end tangentially on one of the disks simplifies the search procedure for them considerably: whereas in the case of geometrical n-bounce cycles one had to minimize a function of n bouncing parameters, we here only have one parameter in play, namely the angle where the creeping orbit leaves the initial disk. Suppose now that we want a specific creeping orbit described by a series of disk bounces plus the specification of the final creeping domain as above. We then scan through all the angles that leave the first disk in the fundamental domain. This gives us an interval of angles where the first wanted disk is being hit. We then scan this interval for bounces on the next disk in the itinerary and so on. Finally we scan the last obtained interval to find the angle under which the ray creeps into the wanted side of the final disk. Having obtained the creeping cycles we can calculate the effective radius by using the usual Jacobian (2.12) for the stabilities. In table 6.2 we list the data for the first few creeping cycles.

To evaluate the results of the diffraction extended Gutzwiller-Voros spectral determinant, we compare the resonances determined by this, to the resonances determined just from geometrical orbits and to the exact quantum resonances.

The data are displayed in fig. 6.9. As one can see the Gutzwiller Voros determinant accounts reasonably well for the leading order of resonances, whereas it fails for the next series. In fig. 6.9, however, we can see that – when a few periodic creeping orbits are introduced – the results are *qualitatively different*, and represent much better the trend of the exact quantum resonance data. For instance, one can make a one-to-one identification of the quantum and semiclassical resonances, which is not possible in the purely geometrical theory, since in that approximation even the number of resonances is wrong.

The series of subleading resonances also approximately defines the lower boundary of the region in which the diffractional spectral determinant still has a high accuracy and good convergence properties. This can also be seen from fig. 6.9 since for small Re k and large negative Im k we have a relatively larger deviation between the exact and creeping resonances.
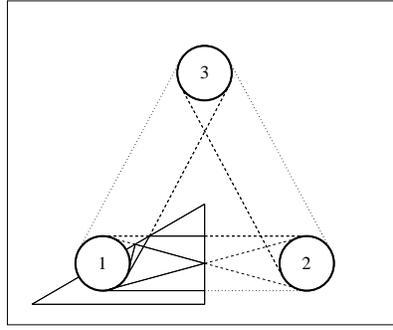
Figure 6.8: The full 3-disk system with a copy of the fundamental domain. Representatives of the creeping orbits of topological length 1 are displayed in full space as well as in the fundamental one.
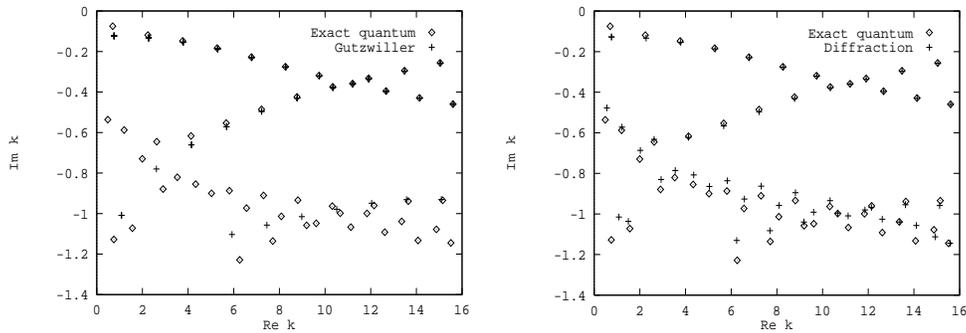

Figure 6.9: (Left) The exact quantum mechanical resonances (diamonds) and the pure geometrical Gutzwiller Voros resonances (crosses) in units of $1/a$ in the complex k plane. The resonances belong to the one-dimensional A_1 representation of the 3-disk system with $R{:}a = 6$. In the semiclassical calculation cycles up to topological length 4 have been used. The leading resonances close to the real axis are described well by the Gutzwiller Voros resonances whereas the subleading semiclassical resonances clearly deviate from the exact quantum resonances. (Right) The exact quantum mechanical (diamonds) and the semiclassical (crosses) A_1 resonances of the $R{:}a = 6$ three-disk system. The resonances are calculated by including diffractional creeping orbits up to order 4 in the geometrical theory of diffraction. As in the two disk case an improvement of the approximation is clearly visible, especially for the second row of the leading resonances as well as for the subleading diffractional ones. In the latter case the qualitative trend is clearly reproduced. As discussed above, the accuracy of the semiclassical resonances becomes worse in the region where Re k is small and Im k is large.

p_c	R_b^{eff}/a	L_b^G/a	L_b^D/a
12	6.000000	6.000000	4.188790
12	5.656854	5.656854	3.821266
13	6.000000	6.000000	2.094395
13	5.656854	5.656854	3.821266
121	58.167840	9.832159	4.523686
121	58.787753	9.797958	3.544308
131	58.167840	9.832159	2.429291
131	58.787753	9.797958	3.544308
123	66.352162	10.120809	4.384819
123	73.492203	10.147842	3.478142
132	84.855171	10.120809	2.678761
132	73.492203	10.147842	3.478142

Table 6.2: Creeping cycle data for the 3-disk system with $R : a = 6$. The first column indicates the itinerary of the orbit, second column the effective radius of the orbit calculated by means of the Sinai-Bunimovich curvatures and finaly the third and fourth columns shows the length of the free flight and the creeping sections respectively.

6.5.3 Corrections to the Airy approximation

In our calculation of the diffractive Greens function G_{creep} we used the Airy approximation (6.43) for the Hankel functions and its zeros. This approximation is only the leading term in a polynomial series of corrections to the zeros. In reference [28] and especially in Franz and Galle [29] one can find correction terms to order $\mathcal{O}((ka)^{-5/3})$ to the standard Airy approximation of the zeros ν_l of the Hankel function $H_\nu^{(1)}(ka)$ in the complex plane. These corrections read
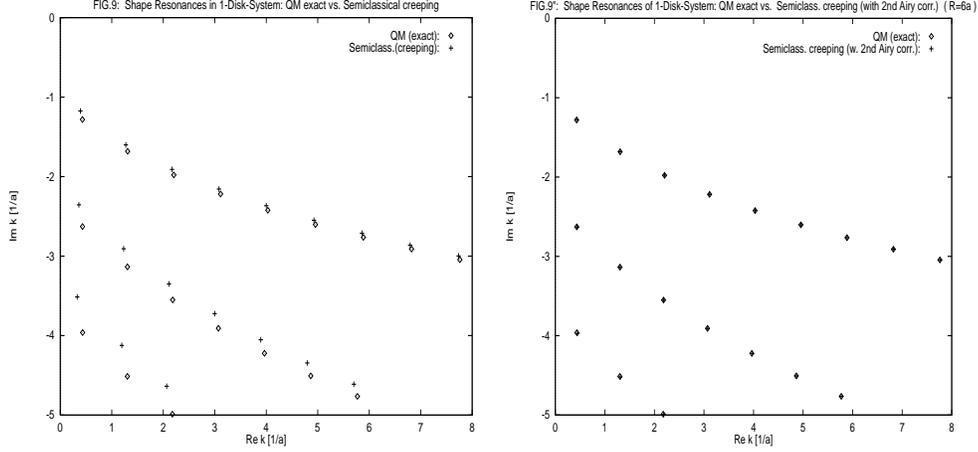
Figure 6.10: (Left) The exact quantum-mechanical resonances for the 1-disk scattering system (given by the zeros of $H_m^{(1)}(ka)$) are plotted as diamonds, the diffractional semiclassical resonances which are given by the zeros of the creeping determinant $\Delta_{1-disk}(k) = \prod_{l=1}^{\infty}(1 - e^{i\nu_l 2\pi a})$ are plotted as crosses. In this calculation only the standard Airy approximation is used. Note that the creeping terms to this order systematically underestimate the magnitude of the imaginary part of the exact resonances. We also see that the semiclassical data becomes better with increasing real part of the wave number k, and with decreasing $|\mathrm{Im}k|$, as they should as semiclassical approximations. (Right) The same as above figure except that the semiclassical resonances now include the two first terms up to order $\mathcal{O}((ka)^{-1})$ in the Airy corrections. We see that the approximation is almost perfect, especially for the leading row of resonances. The inclusion of the 3rd Airy correction (terms of order $\mathcal{O}((ka)^{-5/3})$) does not change the plot further. The data are from A. Wirzba.

$$
\begin{aligned}
\nu_l \;=\; & ka + e^{i\pi/3}(ka)^{1/3}s_l \\
& -e^{-i\pi/3}(ka)^{-1/3}\frac{s_l^2}{30} \\
& -\frac{(ka)^{-1}}{70}\left(1 - \frac{s_l^3}{5}\right) \qquad\qquad\qquad (6.93)\\
& +e^{i\pi/3}\frac{(ka)^{-5/3}}{3150}\left(29s_l - \frac{281s_l^4}{180}\right) \\
& +\ldots, \qquad\qquad\qquad\qquad\qquad\qquad (6.94)
\end{aligned}
$$

where $s_l = 6^{-1/3}x_l$, and x_l is the l'th zero of the Airy integral $Ai(x) = \int_0^\infty dt \cos(xt - t^3)$. The standard Airy approximation only contains the first two terms in the above series and therefore is only of order $\mathcal{O}((ka)^{1/3})$. Wirzba [64] has studied the influence of these corrections in the simple case of the 1- and 2-disk scattering systems. As can be seen from figure 6.10, it turns out that the corrections improve the pure creeping results considerably. For the 2-disk scatterer a similar improvement of the resonances are observed by inclusion of the next terms in the Airy approximation.

As seen from the numerical results it would be very nice if one could incorporate the Airy corrections into our expression for the creeping propagator. This however is not so straightforward in the general case as in the 1-disk situation. The reason is that it is not sufficient to include the Airy corrections in the decay exponents α_l, since one should also include the changes in ν_l in the Debye approximation, which makes the previous so clear geometrical interpretation of the ingredients of the propagator more ambiguous. The improvements in the results are though quite dramatic, so it seems worthwile to try to find the analog in the Keller construction. However, this still remains to be done.

6.6   Discussion

In this chapter we have derived a method to obtain a semiclassical approximation to the quantum propagator including certain diffraction effects such as diffraction along smooth surfaces as well as diffraction from vertices. The method is based on the geometrical theory of diffraction introduced by Keller. We have shown how the introduced periodic creeping orbits inflict on the Gutzwiller trace formula and we have constructed a scheme on how to incorporate the diffraction effects in the semiclassical spectral determinant for quantum systems. By numerical computations we have furthermore shown that by inclusion of the diffraction effects the semiclassical resonances of simple scattering systems changes dramatically and describes very well the exact quantum resonances. As the description is semiclassical we use the Van Vleck propagator for the free flight sections and our semiclassical approximation to the creeping propagator for the creeping sections. The errors of the resonances entering by this approach are therefore mainly originated in three sources:

1. To be able to keep our calculation in terms of basic primitive cycles we used only the $l = 1$ mode in the semiclassical approximation to the creeping propagator. This approximation is justified when the real part of ka is of order of, or larger than 1, since the exponential damping term $\alpha_l(k)$ goes like

$$\alpha_l(k) \quad \simeq \quad const \times \text{Re } (ka)^{1/3}(l - \frac{1}{4})^{2/3} \tag{6.95}$$

and the relative error thus introduced is less than 1 percent for $ka \leq 2$. This error is therefore not sufficient to explain our deviations from the exact resonances.

2. In our semiclassical evaluation of the creeping propagator we use the Airy approximation. As it was demonstrated by the calculations of A. Wirzba, the polynomial terms in the Airy corrections can give sizeable corrections to the calculated resonances. In the simpler 1-disk[29] and 2-disk[64] problems the contributions resulting from the higher polynomial terms in the Airy expansion of the creeping propagator move the subleading semiclassical resonances on top of their corresponding exact quantum analogs to

figure accuracy. In the three-disk case the corresponding calculation is plagued by the exponentially proliferating number of periodic orbits, but the hope is of course that the corresponding Airy correction terms could improve the subleading semiclassical resonances as well.

3. Even the cumulant expansion of the exact quantum mechanical scattering determinant is for large negative $\text{Im}\, k$ very delicate as the single terms entering the cumulant expansion become individually large[64]. As the periodic orbit expansion is just the semiclassical approximation to the cumulant expansion [61], it cannot be expected that the periodic orbit expansion works better than this. In fact, as the individual contributions of the periodic orbits become larger with increasing negative $\text{Im}\, k$, the individual errors from the semiclassical expansion are also increasing such that the total error can become sizable.

It would be natural to expect that the exponential proliferation of periodic orbits in the case of the 3-disk system, might destroy the validity of the semi-classical description completely. We conclude that this seems not to be the case. As we have demonstrated, one only need the basic representatives of the creeping families to change the picture of the scattering resonances drastically, in the direction of the exact quantum resonances.